Journal of Structural Engineering and Geotechnics,
2 (2), 29-38, Winter 2012

Numerical Solution of Seismic Wave Propagation Equation in Uniform Soil on Bed Rock with Weighted Residual Method

M.H. Jahangir[a*]

[a]*Assistant Professor, Faculty of New Sciences & Technologies, University of Tehran, Tehran, Iran.*

Received 5October 2012, Accepted 24 November 2012

Abstract

To evaluate the earth seismic response due to earthquake effects, ground response analyses are used to predict ground surface motions for development of design response spectra, to compute dynamic stresses and strains for evaluation of liquefaction hazards, and to determine the earthquake induced forces that can lead to instability of earth and earth-retaining structures. Most of the analytical solutions presented are affected by the defect that the stress-strain relationship must be of rather simple form (linear elastic, with perhaps linear hysteretic damping), and that the soil properties must be homogeneous. Real soils are often composed of several layers of variable properties, and often they exhibit non linear properties. Therefore, a numerical solution may be considered, because this can more easily be generalized to non-linear and non-homogeneous properties. In this paper, a simple numerical solution method is presented, again with damping property. The considerations will be restricted to one-dimensional wave propagation in a linear elastic layer which the equation of motion will be resolved with weighted residual method and the advantages of using this method will be ultimately discussed. Of course, the most important benefit of this element free approach is having a suitable approximated function for wave displacement in height of a soil layer.

Keywords: Ground response, Wave propagation, Numerical solution, Weighted residual method,Element free approach.

1. Introduction

In recent years, the meshless or element free approaches have gained significant popularity. Amongst these diffused element methods [1], the element free Galerkin method [2-4] and the meshless local Petrov–Galerkin method have been more used than the others [5]. A major preference of these approaches is that an unstructured distribution of nodes can be used, and adaptive procedures introducing more nodes in regions of high error implemented easily. However, like the finite element method, the solution of unbounded domains can only be achieved through truncation of the domain of interest at some distance 'sufficiently far' from the region of interest. This led Gu and Liu [6] to develop a coupled element free Galerkin in boundary element method, which allows use of the boundary element method to model the far field of an unbounded domain, while the element free method is used in the near field. To accomplish this, an 'interface region' is introduced which is effectively discredited with finite elements (within which the shape functions transition from standard shape functions on the boundary to element free shape functions at the edge of the interface region) following the approach of Krongauz and Belytschko [7] to the application of essential boundary conditions. Such an approach is somewhat unappealing, as it introduces an element structure which is contrary to the philosophy of an 'element free' approach.The scaled boundary finite element method is a semi analytical method developed relatively recently by Wolf and Song [8-11]. The method introduces a normalized radial coordinate system based on a scaling centre and a defining curve (usually taken as the boundary). Shape functions are introduced in the circumferential direction and the weakened governing differential equations are solved analytically in the normalized radial direction. Like the boundary element method, discretisation of the boundary is only required, but unlike that method no fundamental solution is required. Initially derived to compute the dynamic stiffness matrix of unbounded domains, the method proved far more versatile than initially envisaged, and was extended to static problems and bounded domains. The rather complicated mathematics of the method in comparison with the ubiquitous finite element method hindered uptake of the method by other researchers. A virtual work derivation for elasto-statics [12] increased the transparency of the method considerably, lead to the development of stress recovery and error estimating procedures [13], which in turn allowed adaptive procedures to be implemented [14]. Using these procedures, direct comparison of computational cost for achievement of a prescribed level of accuracy was possible, and the method was shown to be more efficient

*Corresponding Author Email:: jahangir@dena.kntu.ac.ir

than the finite element method for problems involving unbounded domains. The method itself and many of the recent developments are described by Wolf in [15]. Recently a meshless Petrov–Galerkin version of the method has been developed [16]. A significant advantage of the meshless approach is that a continuous approximation can be obtained in the circumferential direction, which, coupled with the analytical solution is obtained in the radial direction, leads to a very smooth solution in which is the derivative quantities (e.g. stresses for elasto-static or elasto-dynamic problems) are continuous. Despite its advantages, the scaled boundary method has certain limitations. By considering the problems of elasto-statics, the variations in material properties must be scalable relative to the scaling centre, while the loads placed on the side faces must follow the power law distributions and the patch load distributions within the domain are not permissible, and the material must behave in a linear elastic manner. In problems involving unbounded domains, such conditions are often violated in the near field. To overcome this limitation, it is often desirable to couple the scaled boundary method with an alternate method to model the near field. For the scaled boundary finite element method, coupling with the finite element method is a straightforward process [17], since the scaled boundary finite element shape functions are compatible with the finite element shape functions, and no discontinuity occurs across the interface. Coupling a meshless method with another technique to model the far field is not straightforward, as the displacement along the boundary is controlled not only by the degrees of freedom at nodes on the boundary, but by degrees of freedom at nodes in the vicinity of the boundary. When the meshless scaled boundary method is coupled with a meshless method for the near field, the perfect continuity of displacements along the interface cannot be maintained, since the displacements in the unbounded scaled boundary domain are controlled only by degrees of freedom on the boundary, while displacements at the boundary in the meshless near field are controlled by degrees of freedom at all nodes in the vicinity of the boundary. This paper proposes a technique coupling the two approaches, while minimizing this problem. The method could be used equally as well to couple meshless methods with other approaches to modeling the unbounded domain, such as the infinite element method and the boundary element method. Discussions in this paper are limited to the one-dimensional wave propagation in a linear elastic layer, although the techniques can easily be generalized to other types of engineering problems and for two or three dimensions.

In this paper, an analysis is presented for the response of a linear elastic layer during an earthquake. The earthquake is supposed to be generated in the base rock underlying the soft soil system. The earthquake generates various waves in the rock, which leads to waves of vertical and horizontal displacements along the rock surface, generating compression waves and shear waves in the overlying soil. In earthquakes, the most important component usually is the wave of horizontal displacements at the rock surface, which generates shear waves in the soil. In this study, some solutions will be presented, mainly for a homogeneous linear elastic layer. The effect of hysteretic damping will also be considered. An important class of techniques for ground response analysis is also based on using the transfer functions. For the ground response problems, transfer functions can be used to express various response parameters, such as displacement, velocity, acceleration, shear stress, and shear strain, to an input motion parameter such as bedrock acceleration. Because it relies on the principle of superposition, this approach is limited to the analysis of linear systems. Nonlinear behavior can be approximated, however, using an iterative procedure with equivalent linear soil properties.

The paper commences with a brief review of the weighted residual method, followed by a review of the wave propagation in uniform, damped soil on rigid rocks. Then, the new technique is developed, and some diagrams are presented illustrating the effectiveness of the approach.

2. Basic equations

2.1. Wave propagation in uniform, undamped soil on rigid rock

One-dimensional ground response of a soil deposit is predominantly caused by SH-waves propagating vertically from the underlying bedrock. For one-dimensional ground response analysis, the soil and bedrock surface are assumed to extend infinitely in the horizontal direction. In this manner, the returned wave from layer boundary will be omitted. To predict the ground response, the procedures based on this assumption have been shown which is in reasonable agreement with measured response in many cases. In this section, the propagation of horizontal vibrations in a column of soil generated by the vertical motion of the base rock is considered. As mentioned above, it is assumed that the problem is one dimensional in each column, with the displacement being a function of the vertical coordinate z and time only.

The basic differential equation is the one dimensional wave equation, which can be shown as follows,

$$\frac{\partial^2 u}{\partial t^2} = v_s^2 \frac{\partial^2 u}{\partial z^2} \quad (1)$$

Where, v_s is the propagation velocity of shear waves which is,

$$v_s = \sqrt{G/\rho} \quad (2)$$

Where, ρ is the density of the soil and G is the shear modulus. For the simplest case, namely that of a homogeneous layer with no surface load, the boundary condition may be supposed to be,

$z=0:\ \frac{\partial u}{\partial z}=0$ (3)

and the initial condition is

$t=0:\ u=0$ (4)

The boundary condition expresses that the top of the soil layer (the soil surface) is free of stress and the initial condition states that the whole soil layer has no displacement at first. The vertical displacement, w has been disregarded, or, to be more precise, so, it has been assumed that the derivative $\partial w/\partial x$ is small, compared to $\partial u/\partial z$. The exact analytical solution of the problem defined by the equations (1), (3) and (4) is,

$u(z,t)=Ae^{i(\omega t+kz)}+Be^{i(\omega t-kz)}$ (5)

where, ω is the circular frequency of ground shaking, k the wave number ($=\omega/v_s$) and A and B the amplitudes of waves traveling in the $-z$ (upward) and $+z$ (downward) directions, respectively. At the free surface ($z=0$), the shear stress, and consequently the shear strain, must vanish, that is,

$\tau(0,t)=G\gamma(0,t)=G\frac{\partial u(0,t)}{\partial z}=0$ (6)

Substituting (5) into (6) and differentiating yields,

$Gik(Ae^{ik(0)}-Be^{-ik(0)})e^{i\omega t}=Gik(A-B)e^{i\omega t}=0$ (7)

which is satisfied nontrivially when $A=B$. The displacement can then be expressed as

$u(z,t)=2A\frac{e^{ikz}+e^{-ikz}}{2}e^{i\omega t}=2A\cos kz\ \ e^{i\omega t}$ (8)

which describes a standing wave of amplitude $2A\cos kz$. The standing wave is produced by the constructive interference of the upward and downward traveling waves and has a fixed shape with respect to depth. Equation (8) can be used to define a transfer function that describes the ratio of displacement amplitudes at any two points in the soil layer. Choosing these two points to be the top and bottom of the soil layer gives the transfer function like below,

$F_1(\omega)=\frac{u_{\max}(0,t)}{u_{\max}(h,t)}=\frac{2Ae^{i\omega t}}{2A\cos kh\ \ e^{i\omega t}}=\frac{1}{\cos kh}=\frac{1}{\cos(\omega h/v_s)}$ (9)

The modulus of the transfer function is the amplification function as,

$\left|F_1(\omega)\right|=\sqrt{\{\mathrm{Re}[F_1(\omega)]\}^2+\{\mathrm{Im}[F_1(\omega)]\}^2}=\frac{1}{\left|\cos(\omega h/v_s)\right|}$ (10)

which indicates that the surface displacement is always at least as large as the bedrock displacement and, at certain must larger? Thus $\left|F_1(\omega)\right|$ is the ratio of the free surface motion amplitude to the bedrock motion amplitude. As $\omega h/v_s$ approaches $\pi/2+n\pi$, the denominator of equation (10) approaches zero, which implies that infinite amplification or resonance will occur. Even, this very simple model illustrate that the response of a soil deposit is highly dependent upon the frequency of the base motion, and that the frequencies at which strong amplification occurs depend on the geometry (thickness) and material properties (s-wave velocity) of the soil layer. It should be noted that in this section, damping which is an essential property of soft soils, has not been taken into account, and that the considerations refer only to shear waves.

2.2. Wave propagation in uniform, damped soil on rigid rock

In real materials, one part of the elastic energy of a traveling wave is always converted to heat. The conversion is accompanied by a decrease in the amplitude of the wave. Viscous damping, by virtue of its mathematical convenience, is often used to represent this dissipation of elastic energy. For the purposes of viscoelastic wave propagation, soils are usually modeled as Kelvin-Voigt solids. In this paper, the stress-strain relationship for a kelvin- Voigt solid in shear can be expressed as,

$\tau=G\gamma+\eta\frac{\partial\gamma}{\partial t}$ (11)

Where, τ is the shear stress, γ is the shear strain, and η is the viscosity of the material. Thus the shear stress is the sum of an elastic part (proportional to strain) and a viscous part (proportional to strain rate).

Since damping is present in all materials, more realistic results can be obtained by repeating the analysis with damping. Assuming the soil to have the shearing characteristics of a Kelvin-Voigt solid, the wave equation can be written as,

$\rho\frac{\partial^2 u}{\partial t^2}=G\frac{\partial^2 u}{\partial z^2}+\eta\frac{\partial^3 u}{\partial z^2\partial t}$ (12)

The solution to this wave equation is of the form [18],

$u(z,t)=Ae^{i(\omega t+k^* z)}+Be^{i(\omega t-k^* z)}$ (13)

Where, k^* is a complex wave number with real part k_1 and imaginary part k_2. Repeating the previous algebraic manipulations with the complex wave number, the transfer function for the case of damped soil over rigid rock can be expressed as,

$F_2(\omega)=\frac{1}{\cos k^* h}=\frac{1}{\cos(\omega h/v_s^*)}$ (14)

Since the frequency-independent complex shear modulus is given by $G^*=G(1+i2\xi)$, the complex shear wave velocity can be expressed as,

$v_s^*=\sqrt{\frac{G^*}{\rho}}=\sqrt{\frac{G(1+i2\xi)}{\rho}}\approx\sqrt{\frac{G}{\rho}}(1+i\xi)=v_s(1+i\xi)$ (15)

Then the complex wave number can be written, again for small ξ, as,

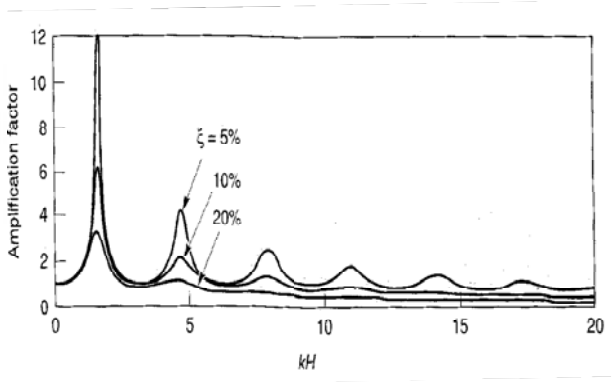

Fig. 1.Influence of frequency on steady state response of damped, linear elastic layer.

And finally, the amplification function can be simplifiedto:

$$|F_2(\omega)| = \frac{1}{\cos k(1-i\xi)h} \approx \frac{1}{\sqrt{\cos^2 kh + (\xi kh)^2}} = \frac{1}{\sqrt{\cos^2(\omega h/v_s) + [\xi(\omega h/v_s)]^2}} \quad (17)$$

For small damping ratios, equation (17) indicates that amplification by a damped soil layer also varies with frequency. The amplification will reach a local maximum whenever $kh \approx \pi/2 + n\pi$ but will never reach a value of infinity since (for $\xi > 0$) the denominator will always be greater than zero. The frequencies that correspond to the Local maxima are the natural frequencies of the soil deposit. The variation of amplification factor with frequency is shown for different levels of damping in the following figure. This amplification factor is also equal to the ratio of the free surface motion amplitude to the bedrock motion amplitude. As shown in Figure 1, damping affects the response at high frequencies more than lower frequencies**.**

3. Numerical solution

All the analytical solutions presented above suffer from the defect that the stress-strain-relationship must be of rather simple form (linear elastic, with perhaps linear hysteretic damping), and that the soil properties must be homogeneous. Real soils are often composed of several layers of variable properties, and often they exhibit non linear properties. Therefore a numerical solution may be considered, because this can more easily be generalized to non-linear and non-homogeneous properties. In this section, a simple numerical solution method is presented with hysteretic damping. The considerations will be restricted to one-dimensional problems, such as wave propagation in a soft layer, from a stiff deep layer to the ground surface. For this relatively simple class of problems there is a little difference between the various existing numerical techniques, such as finite elements, weighted residual method and finite differences. Therefore, the simplest of these methods, a weighted residual method which is a meshless approach in comparison with the others, will be used.

3.1. Weighted residual method

The finite element process, being the base of the weighted residual approximation, will seek the solution with numerical function in below form,

$$\hat{u}(x,t) = \psi + \sum_{m=1}^{n} a_m N_m(t,x) \quad (18)$$

Where, N_m is the shape function prescribed in terms of independent variables (such as the coordinates x, t.) and all or most of the parameters a_m are unknown, and also, ψ is the initial function that is in terms of time parameter. Until now, this form of approximation was used in the displacement approach to elasticity problems. Also, it is important to know that (a) the shape functions were usually defined locally for elements or subdomains and (b) the properties of discrete systems were recovered if the approximating equations were cast in an integral form. With this object in mind we shall seek to cast the equationfrom which the unknown parameters a_m are to be obtained in the integral form,

$$\int_0^h \int_0^t w_l \left(v_s^2 \frac{\partial^2 u}{\partial z^2} - \frac{\partial^2 u}{\partial t^2} \right) dt dz + \int_0^t w_l \left(\frac{\partial u}{\partial z} - 0 \right)_{z=0} dt + \int_0^h w_l (u-0)_{t=0} dz = 0 \quad (19)$$

in which, v_s prescribe known constant that names propagation velocity and w_l is the weighted function of the residual integral which can get it equal to shape function. Thus, Galerkin method is used to selecting of the weighted function.

These integral forms will permit the approximation to be obtained element by element and an assembly to be achieved by the use of the procedures developed for standard discrete systems, since, providing the function u is integral able, by using the equation (18) we have,

$$\sum_{l,m=1}^{M} \left[\begin{array}{l} \int_0^h \int_0^t N_l \left(V_s^2 \frac{\partial^2 N_m}{\partial z^2} - \frac{\partial^2 N_m}{\partial t^2} \right) a_m dt dz \\ + \int_0^t N_l \left(\frac{\partial N_m}{\partial z} \right)_{z=0} a_m dt + \int_0^h (N_l N_m)_{t=0} a_m dz \end{array} \right] - \int_0^h \int_0^t N_l \frac{\partial^2 \psi}{\partial t^2} dt dz + \int_0^h (N_l \psi)_{t=0} dz = 0 \quad (20)$$

Then the approximating above equation will yield a set of linear equations of the below form,

$Ka = f$ (21)

Where,

$$K_{lm}=\sum_{m=1}^{M}\left[\begin{array}{l}\int_0^h\int_0^t N_l\left(v_s{}^2\dfrac{\partial^2 N_m}{\partial z^2}-\dfrac{\partial^2 N_m}{\partial t^2}\right)a_m dtdz\\ +\int_0^t N_l\left(\dfrac{\partial N_m}{\partial z}\right)_{z=0} a_m dt+\int_0^h\left(N_l N_m\right)_{t=0} a_m dz\end{array}\right] \quad (22)$$

and,

$$f_l=\int_0^h\int_0^t N_l\frac{\partial^2\psi}{\partial t^2}dtdz-\int_0^h\left(N_l\psi\right)_{t=0}dz \quad (23)$$

Here simply, the original shape (or basis) functions are used as weighting.

A further point concerning the coefficients of the matrix K should be noted here. The third part, comes from initial condition, is symmetric but the second corresponding to the pure wave propagation equation is not and thus a system of non-symmetric equations needs to be solved. Furthermore, by considering the exact answer at analytical solution, the shape functions must be selected in frequenting math form. Of course, the inherent nature of seismic wave propagation is frequentative phenomena too. Thus, the trigonometric functions are the best choices for substituting of shaped functions.

A computer program using the method described here should be used as an alternative to the analytical solution presented in this paper, and may be used as a basis for more general problems, of homogeneous layers, and perhaps involving non-linear soil properties. When comparing the results of a simple computer program with the analytical results it will be observed that there may be considerable deviations, especially for small values of time. This is a result of the initial condition in the numerical solution. It may take many cycles of vibrations before the numerical solution has reached the steady state that has been assumed in the analytical solutions. Actually, during a real earthquake the soil may not reach the steady state, and the results of a non-steady computation may be more realistic.

3.2. Numerical example

In the present section, a numerical example is considered,illustrating the potentialities of the proposed formulation. In thefirst part, the simulation of a one-dimensional horizontal displacement is focused,and a soil layer is analyzed taking into account differentshape functions in numerical solution. In the second term, the amplification function can beproduced for two different conditions of soil layer with damping and without it. The results obtained by the present work formulationare compared with analytical answers, whenever possible, or withother methodologies results.

For all results, the propagation velocity can be related to the shear modulus G and the mass density ρ of the soil by the equation (2). The normal value of the shear modulus of sandy soil is of the order of magnitude of $G\approx 30\ GPa$, and the normal value of the density is of the order of magnitude of $\rho\approx 1700\ kg/m^3$.

In this stage, the number of terms in total approximating expression for displacement is considered n=4. Thus, the horizontal vibration in displacement form can be illustrated at two points of a layer height 10m versus time history until to 100sec. Also, the below shape function is used for reduce the residual weighted integral.

$$N(k)=cos(k\pi x).sin(k\pi t+\pi/2) \quad (24)$$

As shown in Fig. 2, it is obvious that for a uniform layer without damping property, the variation of vibration must be in range of united displacement because of using a trigonometric form instead of shape function of numerical solution and also the initial function that is in terms of time parameter, is considered as,

$$\psi=sin(t) \quad (25)$$

Thus, without considering damping factor, it was expected that the variation of displacement on both depth must be adapted on each other and this is free form height of soil layer

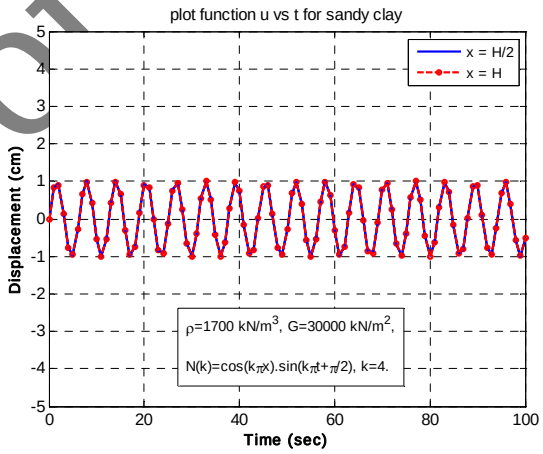

Fig. 2. Horizontal displacement time history at the middle and bottom of the soft layer.

According to Fig. 3, also in variation of displacement versus height, the periodic behavior is achieved becauseof selecting the sine part in shape function due to nature of propagation wave in soft soil. Of course, it should be attended that horizontal displacements at surface level for two different time t=10sec and t=20sec, are begun with various values because of periodic part of depth by using cosine function

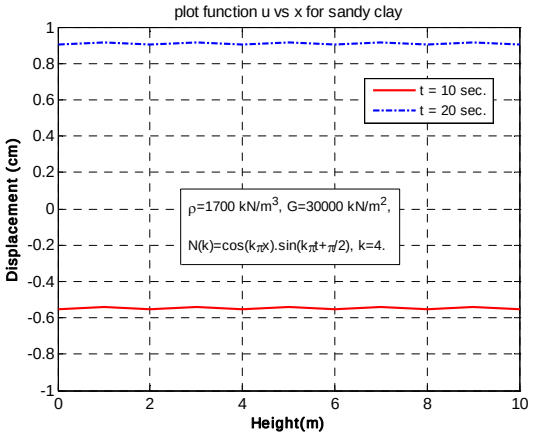

Fig. 3. Horizontal displacement at any height of the soft layer for t=10sec and t=20sec

In both above figures, all result points are adapted on the analytical solution of the wave equation because of its numerical approach in represent of response formulation by polynomial form. Thus, for any height and time, there is a approximate response by this method which is near the exact answer.

3.3. Using different shape functions

In the numerical solution, by changing the x-part uses sine, cosine and tangent function as an activate function; it would be have a better output. Of course, it should be attend that the other math functions can be used as activate function in reducing the residual integral, but due to nature of wave equation, it must be only used the periodic functions as shape function.

The amplification is here regarded in terms of the so-called "amplification function", which is the ratio between the response spectrum (for no damping) of the resulting motion at the surface receiver and the response spectrum of the input motion at the base of the profile (twice the incoming wave field, as would occur at a free surface of the same rock). Fig. 4 shows the variation of amplification with height of soil layer. With a glance to the shape function, it is understood that the amplification can vary with time parameter and the thickness of soil layer (h). By analytical processing, it can be found that the maximum value of amplification (resonance) occurs when $k\pi x=(n-\frac{1}{2})\times\pi$ in which $n=1,2,3,\ldots$. When $n=1$ in particular, the period of resonance is $x=\frac{1}{2k}$, which is very important in seismic microzonation. Thus, when k becomes greater for better approximating, the period of resonance is became smaller and the repetition will be more. Hence, in Fig. 4, by changing the value of k from 4 to 5, this matter can be seen.

The amplification means that the surface motion is $F(\omega)$ times greater than the motion at the base. Although Fig. 4 suggests an infinite value of amplification at resonance, the reality does not cause infinite intensity of surface motion upon (small) motion at the base. Real soil and ground have many kinds of energy loss and does not enable such a strong motion.

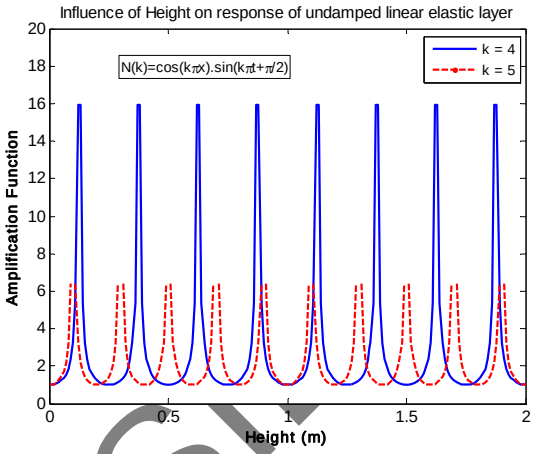

.

Fig. 4. Influence of height on steady state response of undamped, linear elastic layer.

Fig. 5 compares the spectral amplifications of ground motion with respect to the height, obtained by the two another different shape function, for the two values of k . As can be seen, good results are obtained by the maximum values are not reached at the same places at resonance.

The discrepancy among the three curves is due to difference of shape function ratio to x parameter. The location of maximum amplification areas is also very different : in the first case, amplification is occurred in the smaller height, in the second case, amplification is happened in the middle of height in the first and third case, and the maximum amplification is belong to the third case with tangent shaped function. These results show the importance of suitable selecting of shape function proportionate to mechanical characteristics of the soil layers. These characteristics are mean parameters estimated experimentally.

Figs. 4 and 5 indicate that the amplification of the seismic motion reaches a maximum value of 50 for frequencies between 0.196 and 0.785 of height. The highest amplification occurs in the tangent part of shape function for high frequencies, and then in the cosine part around smaller ones. These results are in good agreement with the frequency values determined analytically in section 2.2 (equation 10).

These results further demonstrate that the weighted residual method with the proposed high-order shaped functions is numerically accurate and stable. The amplification level computed with the weighted residual model is much higher than that estimated analytically. The numerical estimation of the amplification factor is three times higher than in the analytical case.

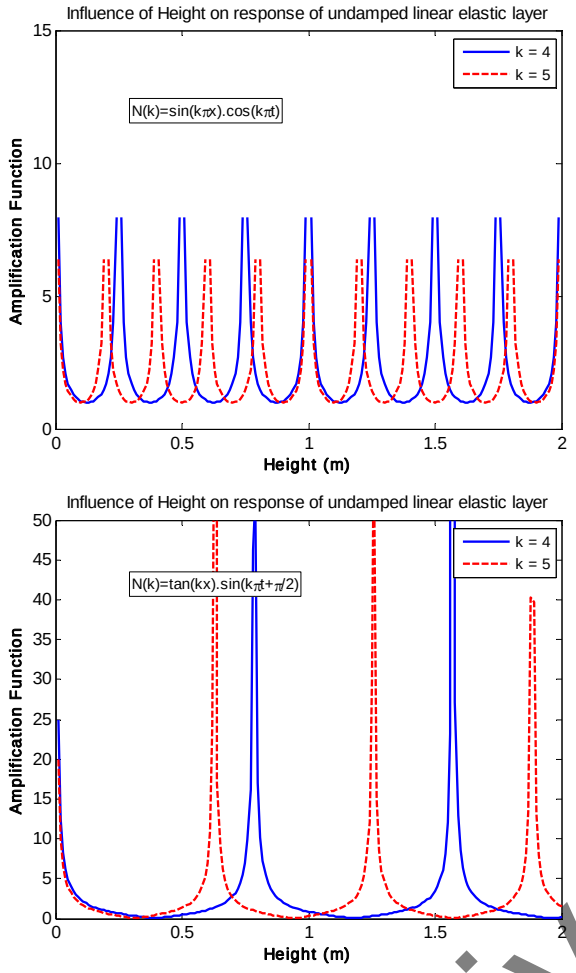

Fig. 5. Influence of height on steady state response of undamped, linear elastic layer.

3.4. Effects of shear velocity

The transfer function results for a sandy clay layer are shown in Fig. 6. As shown in this Fig. , the amplification of the displacement amplitude takes place at distinct frequencies. These frequencies increase as the soil shear wave velocity increases. To evaluate the frequency characteristics of each transfer function, the frequency axis was also normalized using soil column frequency f, which was obtained from the following relationship analytically:

$$f = \frac{v_s}{4H} \quad (26)$$

In the above equation, v_s is the soil shear wave velocity and H is the height of soil deposit. The amplitude of soil displacement at low frequency was used to normalize the amplitude of the displacement transfer functions for all frequencies.

The normalized transfer functions are shown in Fig. 7. As can be seen, the amplification of displacement and its frequency characteristics are about the same for the range of the shear wave velocities considered. In all cases, the maximum amplification takes place at the frequency corresponding to the soil column natural frequency.

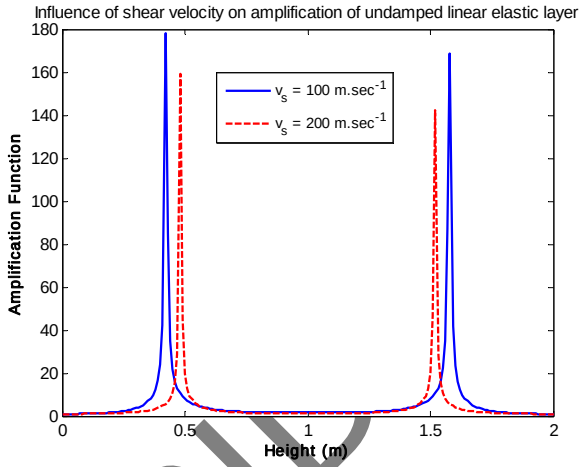

Fig. 6. Typical transfer functions for soil displacement amplitude.

The same dynamic behavior was also observed for all soil elements along the height of the sandy clay layer. Examining the dynamic characteristics of the normalized displacement amplitudes (such as those shown in Fig. 7), it is readily evident that such characteristics are those of a single-degree-of freedom (SDOF) system. Each response begins with a normalized value of one, increases to a peak value at a distinct frequency, and subsequently reduces to a small value at high frequency. Dynamic behavior of an SDOF system is completely defined by the mass, stiffness, and associated damping constant. It is generally recognized that response of an SDOF system is controlled by stiffness at low frequency, by damping at resonant frequency, and by inertia at high frequencies.

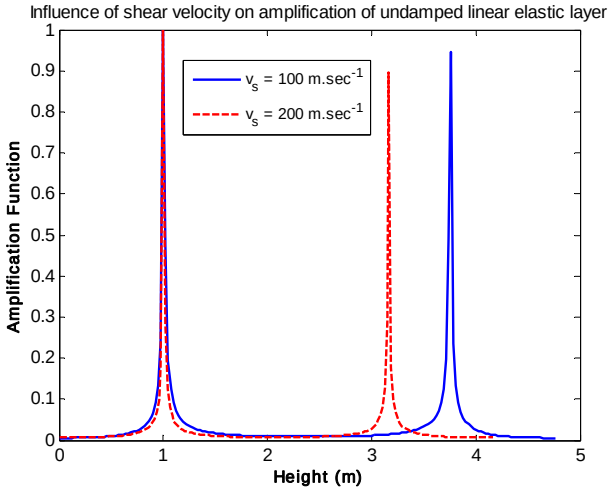

Fig. 7. Normalized transfer functions.

Following the analogy for an SDOF system and to characterize the stiffness component, the displacement amplitudes at low frequencies for all soil elements were obtained. The displacement amplitudes at low frequency are almost identical for the wide range of the soil shear

wave velocity profiles considered, due to the long wave length of the scattered waves at such low frequencies. The shape of the normalized displacement was used as a basis for determining seismic soil displacement along the height of the embedded wall.

3.5. Using different initial functions

According to used method, the ultimate results of displacement are formed from two main parts, the shape and initial function. Despite of major effects of shape functions in ground response, the initial functions also affect on quality of initial conditions in seismic motions. The five different initial functions were used in Fig. 8 compares the surface displacement ratio to layer height in form of time history calculated with the numerically obtained free field motion. Of course, in selecting of these functions, it must be considered that they all are continuous functions in term of time parameter and have the zero value at first of vibration in t=0. As can be seen, there exists an excellent agreement with changing of initial functions. Also, with passing time, the effects of initial functions will be negligible, but in one case, the sine initial function will has its own periodic act.

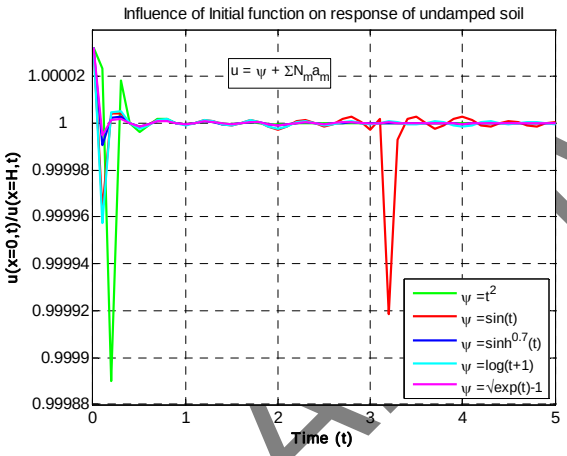

Fig. 8. Variation of amplification with different of initial functions.

The effects of changing initial functions can be appeared in variation of layer height. The numerical model allows the analysis of sensitivity to this parameter. By using the below shape function and varying the initial function ψ, the variation of displacement at start of seismic motion can be compared with ones at t_2=5sec in Fig. 9.

(27), $N(k)=cos(k\pi x).sin(k\pi t+\pi/2)$

In comparison withthe analytical method, the numerical solution has no unknown coefficients and will satisfy initial conditions by choosing a fitting function as ψ. According to Fig. 9, it will be understood that with applying some initial functions, the variation of $u(x,t_1)/u(x,t_2)$ respect to x parameter is approximately equal. But by selecting the sine or logarithmic functions as ψ, the abovementioned expression changes periodic form by different period value. Of course in analytical solution, it can rewrite as below form that can be varied in periodic shape respect to distance x.

$$\frac{u(x,t_1)}{u(x,t_2)}=e^{i\omega(t_1-t_2)} \quad (28)$$

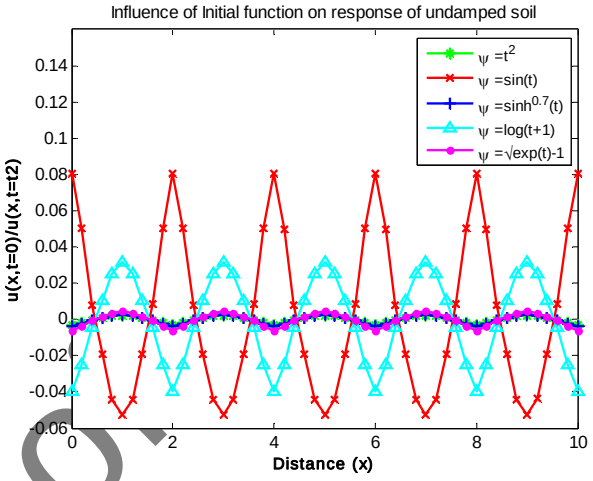

Fig. 9. Variation of displacement ratio to two different time with changing the initial functions.

4. Amplification function with damping

Numerical solution of amplification function for fixed values of equivalent stiffness and damping ratio is plotted in Fig. 10. In this Fig. , the variation of amplification function versus height of soil layer is shown by two different shape functions such as below forms:

$N(k)=(sin^2(k\pi x)+(\xi k\pi x)^2)^{0.3}.cos(k\pi t)$ (29)

and,

$N(k)=(\cos^2(k\pi x)+(\xi k\pi x)^2)^{0.3}.sin(k\pi t+\pi/2)$ (30)

Hence, by changing the above functions in numerical solution, with a fixed value for damping ratio of ξ=0.05, the amplification of displacement transforms from large range values to zero variation by increasing in height of layer, and with using the higher coefficient k in shape functions, the values of periodic height will be reduced. Thus, it is found that changes in shape functions do not affectamplified responses.

As shown in Fig. 10, the amplification of the displacement amplitude takes place at distinct frequencies. The first peak value is called the peak amplification A_p and the corresponding frequency which the predominant frequency v_p. So, how would changes in stiffness and damping affect this amplification function? Parametric study of dependency of the predominant

frequency v_p and the peak amplification A_p on equivalent stiffness and damping ratio is plotted in Fig. 11 for the .

fixed shape function.

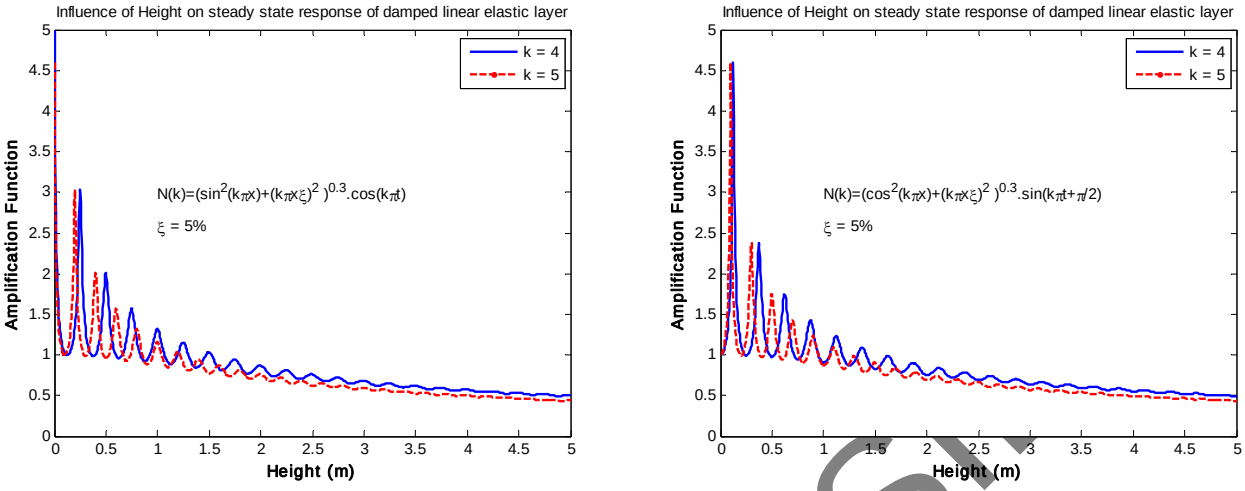

Fig. 10. Numerical solution of amplification function with damping ratio by different shape function N(k).

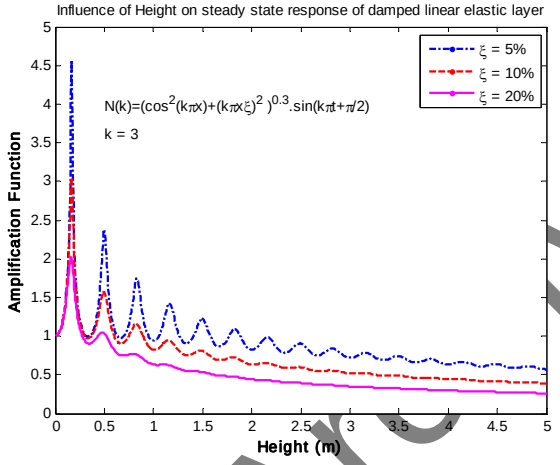

Fig. 11. Variation of amplification function by changing damping ratio

In Fig. 11 the peak amplification is plotted versus the height of the layer. The following conclusions can be drawn from this plot:

1. The peak amplification decreases when the height of the layer increases.
2. For smaller values of damping, the peak amplification increases faster than for larger ones.

The general important conclusion can be known by comparing Fig. s 10 and 11:

For smaller values of the coefficient k in shape function, the peak amplification increases slower than for larger ones.

At very small strains, where the values of damping are small and values of stiffness are large, the peak amplification is more sensitive to errors in damping prediction than in the coefficient k in shape function.

However, for the lowest attenuation value, the discrepancy between damped and undamped curves is not very large. Near the so-called resonance of the soil layer, the influence of damping on amplification can be very strong for high attenuation values. For both frequencies, there is still no significant effect on the location of the peaks.

5. Conclusion

All numerical approaches to solve the differential equations use approximations to the exact calculus expressions. These approaches typically substitute an approximate formula that can be used to estimate some quantity such as a derivative or integral that cannot be found by conventional methods. In the solution of partial differential equations, the approaches convert the differential equation and boundary conditions into a set of simultaneous linear or nonlinear algebraic equations. As the process always leads to equations which, being of integralforms can be obtained by summation of contributions from various sub domains, we decided to embrace all weighted residual approximations under the name of generalized finite element method. In this study, the weighted residual method is used to solve numerically the wave propagation equation in uniformed soil layer on rigid rock. In the paper, we have discussed how approximate solutions can be obtained by using an expansion of the unknown function in terms of trial or shape functions. Further, we have stated the necessary conditions that such functions have to fulfill so that the various integrals could be evaluated over the domain.

Numerical simulations based on the weighted residual method allow a precise description of the site as well as

an accurate analysis of seismic wave propagation within the linear elastic layer. Amplification levels and occurring frequencies are of the same order as the experimental values.

Site effects quantified numerically are sensitive to incidence. It changes the maximum amplification factor, the frequency at which it occurs and the corresponding location. The influence of damping on amplification is also large. Two types of interpretation of this strong influence could be proposed: the first one in terms of vibration and resonance considering that the influence of damping near the resonance of a system is large, the second one in terms of wave propagation taking into account the multiple wave reflections in the soil layer increasing consequently the effect of damping.

To improve the weighted residual method, two main points should be emphasized: the description of the different shape functions with variable soil characteristics and the influence of their respective damping features. These two points may lead to a better understanding of seismic site effects and allow more detailed comparisons between experimental and numerical results. Nevertheless, the experimental determination of dynamic mechanical properties is often difficult (costly, many different methods (cyclic, dynamic...), scattered values) especially when analyzing their distribution with both depth and time along a complete geological profile.

References

[1] B. Nayroles, G. Touzot, P. Villon, "Generalizing the finite element method: diffuse approximation and diffuse elements", Comput. Mech. 10 (1992) 307–318.

[2] D. Organ, M. Fleming, T. Terry, T. Belytschko," Continuous meshless approximations for nonconvex bodies" by diffraction and transparency, Comput. Mech. 18 (1996) 225–235.

[3] T. Belytschko, Y.Y. Lu, L. Gu,"Element-free Galerkin methods", Int. J. Numer. Methods Engrg. 37 (1994) 229–256.

[4] T. Zhu, S.N. Atluri," A modified collocation and penalty formulation for enforcing essential boundary conditions in the element free Galerkin method", Comput. Mech. 21 (1998) 211–222.

[5] S.N. Atluri, T. Zhu, "A new Meshless local Petrov–Galerkin (MLPG) approach in computational mechanics", Comput. Mech. 22 (1998) 117–127.

[6] Y.T. Gu, G.R. Liu, "A coupled element free Galerkin/boundary element method for stress analysis of two-dimensional solids", Comput. Mech. 27 (2001) 188–198.

[7] Y. Krongauz, T. Belytschko, "Enforcement of essential boundary conditions in meshless approximations using finite elements", Comput. Methods Appl. Mech. Engrg. 131 (1996) 133–145.

[8] J.P. Wolf, C. Song, "Consistent infinitesimal finite-element cell method: three dimensional vector wave equation", Int. J. Numer. Methods Engrg. 39 (1996) 2189–2208.

[9] J.P. Wolf, C. Song, "Finite-Element Modelling of Unbounded Media", John Wiley and Sons, Chichester, 1996.

[10] J.P. Wolf, C. Song, "The scaled boundary finite-element method – a primer: derivation", Comput. Struct. 78 (2000) 191–210.

[11] J.P. Wolf, C. Song," The scaled boundary finite-element method – a fundamental solution-less boundary-element method", Comput. Methods Appl. Mech. Engrg. 190 (2001) 5551–5568.

[12] A.J. Deeks, J.P. Wolf," A virtual work derivation of the scaled boundary finite-element method for elastostatics", Comput. Mech. 28 (2002) 489–504.

[13] A.J. Deeks, J.P. Wolf, "Stress recovery and error estimation for the scaled boundary finite-element method", Int. J. Numer. MethodsEngrg. 54 (2002) 557–583.

[14] A.J. Deeks, J.P. Wolf, "An h-hierarchical adaptive procedure for the scaled boundary finite-element method", Int. J. Numer. Methods Engrg. 54 (2002) 585–605.

[15] J.P. Wolf, "The Scaled Boundary Finite Element Method, John Wiley and Sons", Chichester, 2003.

[16] A.J. Deeks, C.E. Augarde, "A meshless local Petrov–Galerkin scaled boundary method", Comput. Mech. 36 (2005) 159–170.

[17] J.P. Doherty, A.J. Deeks, "Semi-analytical far field model for threedimensional finite element analysis", Int. J. Numer. Anal. Methods Geomech. 28 (2004) 1121–1140.

[18] Kramer Steven L., "Geotechnical Earthquake Engineering", 1996 by Prentice-Hall, Inc.